High Throughput Repurposing Screen Reveals Compounds with Activity Against *Toxoplasma gondii* Bradyzoites

Taher Uddin[1], Jing Xia[1], Yong Fu[1], Case W. McNamara[2], Arnab K. Chatterjee[2], L. David Sibley[1*]

[1]Department of Molecular Microbiology, Washington University School of Medicine, St. Louis, MO, USA.

[2]Calibr at Scripps Research, La Jolla, California, USA.

[*]Correspondence: Sibley@wustl.edu

KEYWORDS: High throughput screening, toxoplasmosis, chronic infection

ABSTRACT

Toxoplasma gondii causes widespread chronic infections that are not cured by current treatments due to inability to affect semi-dormant bradyzoite stages within tissue cysts. To identify compounds to eliminate chronic infection, we developed a HTS using a recently characterized strain of *T. gondii* that undergoes efficient conversion to bradyzoites in intro. Stage-specific expression of luciferase was used to selectively monitor growth inhibition of bradyzoites by the Library of Pharmacological Active Compounds, consisting of 1280 drug-like compounds. We identified 44 compounds with >50% inhibitory effects against bradyzoites, including several new highly potent compounds several of which have precedent for antimicrobial activity. Subsequent characterization of the compound Sanguinarine sulfate revealed potent and rapid killing against in vitro produced bradyzoites and bradyzoites harvested from chronically infected mice. These findings provide a platform for expanded screening and identify promising compounds for further preclinical development against *T. gondii* bradyzoites responsible for chronic infection.

32 *Toxoplasma gondii* is a widespread parasite of animals that causes zoonotic infections in humans
33 [1]. Serological studies suggest that ~ 1/3 of humans are chronically infected with *T. gondii*
34 worldwide, although prevalence rates vary widely by geographic region [2]. Human infections are
35 caused by ingestion of undercooked meat, harboring tissue cysts, or ingestion of oocysts shed by
36 infected cats [3]. The acute stage of infection is predominated by fast growing tachyzoites that
37 disseminate widely, including to sites of immune privilege like the brain, followed by
38 differentiation into cysts harboring semi-dormant bradyzoites, which divide slowly and
39 asynchronously [4]. Although most infections are only mildly symptomatic and controlled by the
40 immune system, they persist chronically and hence predispose individuals to subsequent
41 reactivation if they become immunocompromised [5]. The current standard of care treatment does
42 not eradicate chronic infection, hence infected individuals remain at risk of reactivation for life.
43 Long known as a cause of congenital infection [6], recent studies highlight toxoplasmosis as a
44 cause of ocular disease due to newly acquired infections in otherwise healthy adults [7]. Frequent
45 and severe outbreaks of ocular toxoplasmosis have been described in South America [8] and India
46 [9, 10], and may occur in other localities. Notably, infection of healthy individuals in South America
47 often leads to severe, recurrent ocular toxoplasmosis [11], with an estimated disease burden of 30
48 million individuals requiring treatment annually in Brazil alone [12]. Additionally, prior
49 toxoplasma infection has been linked to increased cognitive decline in Alzheimer's Disease,
50 although not all studies have conformed this association, likely due to the complexity of risk
51 factors involved [13].
52 Current therapies for treatment of toxoplasmosis rely on inhibition of the folate pathway in
53 the parasite [14]. The standard of care therapy (i.e. sulfadiazine and pyrimethamine) inhibits the
54 rapidly growing tachyzoite stage but has minimal activity on bradyzoites within tissue cysts and
55 consequently does not eliminate chronic infection [15]. Unfortunately, there are also significant
56 adverse effects of this treatment regimen due to intolerance or allergic reactions [16, 17] and
57 contraindication during the first two trimesters of pregnancy [18]. Although drug resistance is not
58 frequently encountered in treatment of toxoplasmosis, some isolates are naturally resistant to
59 sulfonamides due to natural variants in dihydropteroate synthetase, or other molecular
60 mechanisms, thus complicating treatment in some cases [17]. Clindamycin and several macrolide
61 antibiotics have also been shown to inhibit growth in vitro and in animal models [19, 20] and such
62 antibiotics have been used to treat toxoplasmosis in humans [21]. However, these compounds are

63 not specific to the parasite and disrupt the normal endogenous microbiota leading to possible
64 emergence of pathobionts like *Clostridium difficile* [22].
65 A review of the literature of compounds that are clinically approved in humans or animals
66 identified several compounds that inhibit parasite growth in vitro and/or in murine models of
67 toxoplasmosis [21]. For example, repurposing of guanabenz, an FDA-approved drug that interferes
68 with translation, showed activity against acute and chronic toxoplasmosis in mice [23], although
69 this affect was dependent on the strain of mouse [24], and treatment did not eliminate cysts,
70 resulting in rebound after discontinuation [25]. A repurposing screen for inhibition of tachyzoite
71 growth in vitro using the Tocriscreen Total Library, which consists of 1280 biologically active
72 small molecules with confirmed molecular targets, identified multiple compounds that affect
73 dopaminergic and estrogen signaling, including tamoxifen that was shown to act by upregulating
74 xenophagy to restrict parasite growth and cause clearance [26]. Additionally, a number of new
75 investigational compounds have shown an ability to block tachyzoite growth in vitro and during
76 acute infection in animal models, including several that have activity against bradyzoite growth
77 or chronic infection [17].
78 The majority of efforts to identify new compounds with activity against *T. gondii* have
79 focused on in vitro assays using tachyzoite growth as a readout [17, 21]. Differentiation of
80 bradyzoites in vitro can be achieved by treatment with stress, such as high pH [27]; however, the
81 stages that develop under stress often continue to express tachyzoite markers [28, 29],thus
82 complicating screening efforts. Nonetheless, combining dual promoters to drive firefly luciferase
83 in the cytosol of bradyzoites and Nanoluc luciferase (nLuc) that was engineered to be secreted
84 into the cyst matrix, allowed evaluation of compounds for selective activity against chronic
85 stages [30]. Another promising development is the recent development of an in vitro system for
86 development of bradyzoites using a specialize KD3 muscle cell line where spontaneous
87 differentiation occurs [31]. Consistent with the lack of available treatments on tissue cysts in
88 chronically infected mice, treatment with pyrimethamine and/or sulfadiazine was not effective in
89 restricting the growth of mature bradyzoites formed in vitro in this system [31]. Hence, this system
90 could provide a useful platform for testing compounds for activity against bradyzoites, although
91 it requires the use of a specialized culture system and the treatment and recovery phase needed
92 for evaluation takes ~ 50 days.

93 As an alternative, we recently described a type II strain called Tg68 that has a high
94 propensity to differentiate into bradyzoite in vitro under condition of stress that include high pH
95 or cultivation in high glutamine, low glucose, that forces metabolism based on glutaminolysis [32].
96 Unlike other type II strains that undergo partial differentiation, Tg68 forms fully mature
97 bradyzoites without associated breakthrough of tachyzoites following stress induction in vitro [32].
98 Here, we engineered this strain to express Firefly luciferase (Fluc) under the control of a
99 constitutive promoter, and separately generated a lines expressing nLuc under the control of a
100 bradyzoite promoter. We used these reporter lines to develop a high throughput screen (HTS) and
101 used it to evaluate the Library of Pharmacological Active Compounds (LOPAC). Several
102 compounds with activity against both stages were identified, providing proof of concept for
103 further HTS projects designed to find new treatments for chronic toxoplasmosis.
104

105 **Results and Discussion**

106 To facilitate HTS using the Tg68 strain, we generated a clonal line of Tg68 constitutively
107 expressing firefly-luciferase (Fluc) under the p*TUB1* promoter (**Figure 1A**). The pTub1:Fluc
108 plasmid also contained a resistant DHFR cassette that was integrated into the genome after
109 electroporation followed by selection with pyrimethamine. Following passage in HFF cells, a
110 cloned line constitutively expressing Fluc was isolated and is referred to as Tg68-pTub1:Fluc.
111 Confluent HFF cells grown in 384-well plates were infected with Tg68-pTub1:Fluc tachyzoites
112 at $2x10^4$ parasites per well, and the infection was allowed to proceed for 72 hr under 5% CO_2 at
113 37ºC (**Figure 1B**). Comparison of Fluc activity between day 3 and day 0 (4 hr postinfection)
114 increased significantly, representing growth of the parasite (**Figure 1C**). In addition, we analyzed
115 Fluc expression from replicate 14 wells, across 5 plates and determined the Coefficient of
116 Variation (CV) for positive wells was 7±3% (**Table S1**). Addition of BRD7929, which targets
117 parasite phenylalanine tRNA synthetase [33], completely inhibited parasite growth at a
118 concentration of 10 μM (**Figure 1D**). Comparison of the luciferase signal from untreated and
119 treated wells from 5 plates demonstrated an average Z′ value of 0.77±0.11 (**Table S1**).
120 Additionally, the Tg68-pTub1:Fluc line demonstrated comparable sensitivity to BRD7929 and
121 atovaquone compared to the reference type II strain TgMe49-Fluc (**Figure 1D**). Taken together,
122 these findings indicate that Tg68-pTub1:Fluc provides a robust readout for HTS of compounds
123 against tachyzoite growth.

124 To expand the use of Tg68 for HTS of compounds with activity against bradyzoites, we
125 generated a clonal line expressing nLuc under control of the p*BAG1* promoter, which is strongly
126 upregulated upon differentiation [34]. The pBAG1:nLuc plasmid also contained a resistant DHFR
127 cassette that was integrated into the genome after electroporation followed by selection with
128 pyrimethamine. Following serial passage in HFF cells, a positive clone was isolated and referred
129 to as Tg68-pBAG1:nLuc. (**Figure 2A**). In previous studies, we have shown that the Tg68 strain
130 undergoes highly efficient differentiation to bradyzoites in alkaline media at low CO_2 in vitro and
131 that it retains a mature bradyzoite profile even at relatively high multiplicities of infection [32].
132 Tg68 also undergoes efficient differentiation when grown in glucose free medium supplemented
133 with 10 mM glutamine, a process that forces glutaminolysis for energy production via the
134 mitochondrion [32]. Confluent HFF cells in 384-well plates were infected with pBAG1:nLuc
135 parasites ($3x10^3$ parasites per well) for 2 hr, followed by washing and shifting to alkaline or
136 glutamine media. Cultures were maintained for 10 days under CO_2-free conditions (ambient air),
137 with media changes on day 3 and 6. On day 6, compounds were added and on day 10 luciferase
138 assays were performed (**Figure 2B**). Expression of nLuc was very low in cultures of tachyzoites
139 and in the initial culture conditions at day 0 (4 hr postinfection) in normal or differentiation
140 media (**Figure 2C**). Expression of nLuc increased dramatically by over 4 logs by day 3 and
141 continued to increase significantly at day 6 and at day 10 (**Figure 2C**). On day 10, analysis of
142 luciferase values from 14 wells showed an optimal Coefficient of Variation (CV) of 10±2% for
143 alkaline media and 7±2% for glutamine media, indicating suitability for high-throughput
144 screening (HTS) (**Table S1**). Treatment with BRD7929 at a concentration of 10 μM completely
145 inhibited growth of the parasites and comparison of nLuc activity from treated and untreated
146 wells revealed a Z′ value of 0.67±0.05 for alkaline media and 0.76±0.06 for glutamine media
147 (**Table S1**). We also compared the potency of BRD7929 and atovaquone under both conditions
148 that induced bradyzoite differentiation (**Figure 2D**). Both compounds showed a reduction in
149 EC_{50} values under glutamine differentiation when compared to alkaline conditions, although this
150 was much more dramatic for atovaquone that showed a > 30-fold shift (**Figure 2D**). The greater
151 potency of compounds in glutamine medium may reflect a decreased ability of the parasite to
152 generate energy stores from glutaminolysis vs. glycolysis as suggested previously by the modest
153 growth defects in knockouts of *T. gondii* hexokinase [35] and glucose transporter 1 [36].
154 Consequently, the use of glutamine medium for bradyzoite development may preferentially

155 reveal compounds that act on the mitochondrion, as is the case for atovaquone that inhibits the
156 bc1 complex [37].
157 The LOPAC library (1157 of 1280 total compounds) was plated in 384 well format and tested
158 for parasite growth inhibition in duplicate using a single concentration of 10 μM in the
159 tachyzoite and both alkaline and glutamine-induced bradyzoite assays. Growth inhibition was
160 averaged from the two replicates and plotted as a Venn diagram summarizing the outcome of
161 each of the three assays (**Figure 3A**). A total of 27 compounds showed selective inhibition of
162 tachyzoite growth without affecting growth in the other assays (**Figure 3A**). The largest number
163 of compounds was identified in the glutamine induced bradyzoite assay, perhaps reflecting the
164 metabolic liability of this growth condition (**Figure 3A**). In total, 21 compounds that inhibited
165 parasite growth in all three assays by 50% or more were identified as Primary Hits (**Figure 3A**).
166 Furthermore, we identified 9 compounds that inhibited bradyzoite growth in both assays by 50%
167 or more but not tachyzoite growth (**Figure 3A**). Finally, we identified 14 compounds that
168 specifically inhibited glutamine-induced bradyzoite growth by ≥ 80%, but were not effective in
169 growth inhibition in the other two assays (**Figure 3A**). Robust validation of the within plate and
170 between replicates was performed through collective calculation of the coefficient of variation
171 (CV) and Z' analysis of assay plates (**Table S2**). Of the 44 Primary Hit compounds defined above
172 (**Figure 3B**), 36 compounds were available in quantity at Calibr and were chosen for further
173 testing (**Table S3**). These 36 compounds were tested in a dilution series and 9 compounds were
174 found to have EC_{50} values of ≤ 2 μM in either tachyzoite and/or bradyzoite assays, thus defining
175 a set of Top Hits (**Table S3, Figure 3B**).
176 We were able to source 8 of the 9 Top HIT compounds from commercial sources while one
177 of the top hit compounds Emetine dihydrochloride hydrate (TgEC50 ~70nM) was not available
178 from commercial sources for further study. The 8 available compounds were tested for
179 cytotoxicity against HepG2 and THP-1 cell lines, along with a control drug, atovaquone (**Figure**
180 **3B**). Most compounds exhibited a favorable selectivity index (SI), which is a measure of the
181 compound's EC_{50} against the parasite compared to the CC_{50} against host cells (**Table 1**).
182 However, a few compounds, namely Idarubicin hydrochloride and MS012, showed high toxicity,
183 while Auranofin and JFD00244 showed modest toxicity towards the cell lines. Auranofin is a
184 gold containing compound that has been approved for treatment of rheumatoid arthritis and it has
185 previously been reported to have activity against several parasites [38]. Consistent with this profile,

186 auranofin has previously been shown inhibit replication of the type I RH strain in vitro, reduce
187 infection in a chicken embryo model [39]and reduce the burden of cysts in chronically infected
188 mice [40]. However, the high level of growth inhibition for HepG2 and THP-1 cells treated with
189 auranofin in the present study would appear to limit the potential of this compound for further
190 clinical development. Additionally, Brefeldin A, which blocks ER to Golgi transport showed a
191 favorable SI in HepG2 cells but not in THP-1 cells (**Table 1**), suggesting that block of protein
192 export has very different consequences on host cell growth in different lineages. As a result,
193 these compounds were excluded from further assays due to their undesirable cytotoxic effects.
194
195 **Table 1 Potency and selectivity of Top Hits**

Compound	Tg68Fluc EC_{50} (Tachyzoite)	Me49Fluc EC_{50} (Tachyzoite)	Tg68nLuc EC_{50} (Alkaline)	Tg68nLuc EC50 (Glutamine)	HepG2 CC_{50}	SI	THP-1 CC_{50}	SI
Diphenyleneiodonium Sulfate	0.01	0.01	0.27	0.06	1.28	96	4.85	365
Sanguinarine Sulfate	0.03	0.01	4.00	1.25	9.44	238	4.34	130
Brefeldin A	0.06	0.05	0.40	0.16	60.00	987	0.07	1
Idarubicin hydrochloride	0.19	0.67	0.30	0.82	0.14	1	0.59	3
T0070907	0.75	0.87	0.64	0.60	18.12	24	21.98	29
MS012	2.46	2.68	0.85	2.23	2.03	1	1.19	0.5
Auranofin	2.75	1.12	0.68	0.38	9.81	4	2.83	1
JFD00244	3.89	3.39	2.88	4.48	16.07	4	2.95	1
Atovaquone	0.16	0.10	2.07	0.06	9.67	62	14.26	91
BRD7929	0.11	0.05	0.22	0.08	6.08	54	2.87	25

196 Values in μM, average of two or more biological replicates,
197 SI = selectivity index (Host cell CC_{50} / EC_{50} Tg68Fluc).
198
199 Although Tg68 undergoes efficient conversion to bradyzoites in vitro, with a transcriptional
200 profile that resemble in vivo bradyzoites [32], it may still lack some of the features of mature tissue
201 cysts. Hence, we tested select Top Hits, along with several reference compounds, against tissue
202 cysts that were harvested from chronically infected mice (**Figure 4A**). For these assays, we used
203 the ME49 EW strain, which produces high numbers of cysts in vivo [46]. As shown in Table 1, the
204 ME49 strain has a very similar sensitivity to the Top Hits and reference compounds, thus
205 validating the choice of strain. Compounds were tested using continuous exposure of ex vivo
206 bradyzoites to $3XEC_{90}$ as measured on tachyzoites. Alternatively, ex vivo bradyzoites were
207 treated at $3XEC_{90}$ for only 4 hr followed by washout to ascertain how irreversibly they might act

208 (**Figure 4A**). All three of the reference compounds BRD7929, atovaquone, and pyrimethamine
209 showed potent inhibition of bradyzoites when used continuously (**Figure 4B**). Although
210 atovaquone and BRD7929 are active on bradyzoites (**Table 1**), the activity of pyrimethamine in
211 this continuous treatment assay is likely because it inhibits the outgrowth of tachyzoites.
212 Consistent with this specificity, pyrimethamine was largely ineffective when used for only 4 hr,
213 indicating it has minimal effects on bradyzoites present at the start of the assay (**Figure 4B**).
214 Similar to pyrimethamine, testing of diphenyleneiodonium and T0070907 in the ex vivo
215 bradyzoite assay revealed that they only work when used in continuous treatment, suggesting
216 their activity is static rather than cidal (**Figure S1**). Diphenyleneiodonium is an inhibitor of
217 NADPH oxidase that separately induces oxidative stress [41]. Previous studies have shown
218 diphenyleneiodonium inhibits growth of *T. gondii* tachyzoites in ARPE-19 cells through the
219 production of ROS [42]. In a separate study, it also showed activity against *P. falciparum* with an
220 EC_{50} of 0.06 nM [43], and it has also been shown to have broad spectrum antibacterial activity [44].
221 T0070907 is an inhibitor of peroxisome proliferator activator receptor γ that induces G2/M arrest
222 and thus has activity against cancer cells [45]. This nuclear hormone pathway is not conserved in *T.*
223 *gondii*, and this compound has not been described to have anti-microbial activity previously, so
224 the potential mechanism of action is uncertain.
225 Atovaquone showed partial inhibition in the washout ex vivo bradyzoite assay, and consistent
226 with previous studies showing it is partially active in reducing cysts numbers during chronic
227 infection in vivo [47]. BRD7929 was highly effective in preventing the outgrowth of bradyzoites
228 even when removed after 4 hr (**Figure 4B**), consistent with previous findings [33]. Testing of the
229 Top Hit Sanguinarine sulfate revealed potent activity in the ex vivo bradyzoite wash out assay,
230 thus confirming it has activity against bradyzoites as well as tachyzoites (**Figure 4B**).
231 Sanguinarine sulfate is a natural product produced by the opium poppy and several other plants
232 and it consists of a benzoquinoline alkaloid [48]. Sanguinarine has anti-inflammatory, anti-tumor
233 and antimicrobial activities and it is thought to act on numerous signaling pathways in human
234 cells [49]. Sanguinarine has been described to be toxic to host cell, thought to be due to its action
235 on Na+/K+ ATPase, although other mechanisms have also been described [48]. Although we did
236 not measure appreciable cell toxicity in our assays, other studies have indicated sanguinarine
237 induces apoptosis or blocks cell growth [49]. Additionally, the LD_{50} in mouse is 18 mg/kg by i.p.
238 injection [49], likely limiting its use in efficacy testing for toxoplasmosis.

239 **Conclusions**

240 The newly discovered Tg68 strain is permissive for bradyzoite differentiation and forms the
241 foundation for the screening protocol in this study. We have developed protocols for HTS of
242 compound libraries that target for tachyzoites and bradyzoites and further validated hits in assays
243 against ex vivo produced bradyzoites. Several of the hits identified in this screen have precedent
244 for being antimicrobial; however, they pose challenges for selectively and lack of toxicity.
245 Nonetheless, the methodology develop here offers promise for future HTS to identify potent and
246 selective leads.

247

248 **Experimental Section**

249 **Compounds and liquid handling.** The LOPAC compound library was plated in a 384-well plate
250 format for primary screening and determination of half-maximal effective concentration (EC_{50})
251 of primary hits by Calibr at Scripps Research (La Jolla, CA). The plates were stored at -80°C
252 prior to use. All liquid handling steps (host and parasite cell seeding, media exchange, compound
253 transfer to assay plates, and addition of luciferase reagents) were carried out in a semi-automated
254 facility to ensure efficient and consistent execution of assays across all replicates (High-
255 Throughput Screening Center, Washington University School of Medicine). Eight top hit
256 compounds and two control compounds, atovaquone (Sigma#A7986) and pyrimethamine
257 (Sigma#46706), were obtained from commercial sources, and follow-up assays were manually
258 performed in-house.

259 **Construction of transgenic parasites and parasite culture.** Tg68 pTub1:Fluc,DHFR parasite
260 lines were generated by utilizing a pre-existing pTub:Fluc plasmid [33], which provides
261 constitutive firefly luciferase (Fluc) expression from the alpha tubulin promoter, and a
262 pyrimethamine-resistant DHFR selectable marker. Tg68 tachyzoites were electroporated with 50
263 μg of the plasmid and subsequently selected using pyrimethamine (3 μM).

264 The plasmid pSAG1:EGFP-DHFR-BAG1:nLuc was constructed by assembling fragments
265 encoding EGFP driven by the *SAG1* promoter, nLuc driven by the *BAG1* promoter, DHFR
266 pyrimethamine resistance marker, and pNJ-26 vector using NEBuilder HiFi DNA Assembly
267 Master Mix (NEB). Tg68 pBAG1:nLuc, DHFR tachyzoites (Tg68pSAG1:EGFP-DHFR-
268 BAG1:nLuc) were electroporated with 50 μg of this plasmid and selected with pyrimethamine (3

269 μM) in order to establish stable parasite lines. Detailed primer information can be found in **Table**
270 **S4**.
271 Stable clones were isolated through limiting dilution, and the expression of the transgene was
272 confirmed by luciferase expression. Clonal transgenic Tg68 tachyzoites were maintained by
273 serial passage in T25 flasks with confluent HFFs in D10 medium (Dulbecco's Modified Eagle's
274 Medium, DMEM; Thermo Fisher, 10% fetal bovine serum (FBS), 2 mM glutamine (Sigma), and
275 10 μg/mL gentamicin (Thermo Fisher)) at 37°C and 5% CO_2.
276 **In Vitro Assays for bradyzoite and tachyzoite growth inhibition.**
277 *Host cell culture and seeding*
278 Human Foreskin Fibroblasts (HFF-1 SCRC-1041, ATCC) cells were cultured in T175 flasks
279 using D10 medium. Prior to seeding the cells to the assay plates, a cell suspension was prepared
280 by treating with trypsin (0.5 g/l porcine trypsin and 0.2 g/L EDTA in Hank's Balanced Salt
281 Solution with phenol red) for 5 min. EC_{50} assays (half maximal effective concentration) were
282 conducted in a 384-well plate format. Confluent HFF cells were seeded 4 days in advance using
283 a Multidrop Combi dispensing 80 uL/well, while stirring the cell suspension at 350 rpm. The
284 plates were stacked in a Cytomat rack on a level surface at room temperature until all plates were
285 completed, and then they were placed in a 37°C incubator with 5% CO_2. To minimize edge
286 effects, only the inner 240 wells of each plate were utilized.
287 *Bradyzoite Primary Screening and EC_{50} Assay*
288 The medium from the HFF cell plates was aspirated using a Biotek ELx405CW, leaving 20
289 μL/well, before infection with parasites. Freshly harvested Tg68pBAG1:nLuc,DHFR parasites
290 (3×10^3) in a 40 μL volume were then added to each well (total volume of 60 μL/well, containing
291 0.1% DMSO in D10) using a Fluotics BXi-50F while stirring the parasite suspension at 350 rpm.
292 The plates were incubated for 2 hr at 37°C in a 5% CO_2 incubator to allow parasite invasion.
293 Afterwards, the culture medium was removed and switched to either 80 μL/well of Alkaline
294 (RPMI 1640 (Sigma, #R6504) containing 1% FBS and 50 mM HEPES (Sigma), adjusted to pH
295 8.2), or Glutamine (glucose-free RPMI 1640 (Sigma, #R1383) containing 1% FBS and 50 mM
296 HEPES (Sigma), 10 mM glutamine, adjusted to pH 7.2) medium. The culture was then incubated
297 at 37°C in ambient CO_2 and maintained for 10 days, with media changes occurring on day 3 and
298 6 using a Biotek ELx405CW and Multidrop Combi inside a biohood to minimize contamination.
299 On day 6, before the compound was added, the plates were aspirated, and 40 μL/well of fresh

300 media was added, followed by the transfer of 40 µL/well of 2X compound using a Fluotics BXi-
301 50F. On day 10, the plates were equilibrated to room temperature for 30 min prior to the assay
302 readout. To read the plates, the medium was aspirated, 20 uL of Promega Nano-Glo reagent
303 (Promega N1150) was dispensed into each well using a Multidrop Combi, and the plates were
304 covered with a black lid. The plates were then incubated for 10 min at room temperature, and the
305 readout was performed using Envision.
306 *Tachyzoite Primary Screening and EC_{50} Assay*
307 Before being infected with parasites, the medium was removed from the HFF cell plates using a
308 Biotek ELx405CW, leaving 20 µL/well. Freshly harvested Tg68pTub1:Fluc parasites (2×10^4) in
309 a 20 µL volume were then added to each well while stirring the parasite suspension at 350 rpm,
310 and 40 µL of 2X compound solutions were transferred (80 µL/well total volume, containing
311 0.1% DMSO in D10) using a Fluotics BXi-50F. The plates were incubated for 72 hr at 37 °C in a
312 5% CO_2 incubator. Before the assay readout, the plates were equilibrated to room temperature for
313 30 min. To read the plates, the medium was aspirated to 20 µL using a Biotek ELx405CW, 20 µL
314 of Promega Bright-Glo reagent (Promega E2650) was dispensed into each well, and the plates
315 were covered with a black lid. The plates were then incubated for 10 min at room temperature
316 using a Multidrop Combi, and the readout was performed using Envision.
317 **In Vitro Assays for Host cell cytotoxicity.** Cytotoxicity against host cells host cells was tested
318 using human hepatocellular carcinoma cells (HepG2, ATCC-HB-8065) and human monocytic
319 tumor line (THP-1, ATCC-TIB-202), which were maintained according to ATCC
320 recommendations. Host cell lines were tested negative for mycoplasma using an e-Myco plus kit
321 (Intron Biotechnology). Compounds were diluted to 2X concentration, and a 10-dose serial
322 dilution series was prepared through stepwise, 3-fold dilutions in recommended media with 0.1%
323 DMSO. Host cells were seeded at a density of 10^4 cells/well (100 µL vol) to achieve sub-
324 confluent monolayers for a 72 hr growth assay. Prior to compound addition, THP-1 cells were
325 treated with 10 ng/mL phorbol 12-myristate 13 acetate for 24 hr to facilitate differentiation into
326 macrophages. HepG2 cells were treated with compounds 6 hr post-seeding (200 µL final volume,
327 0.05% DMSO) and incubated under 37 °C, 5% CO_2 culture conditions. At 72 hr post compound
328 addition, culture media were aspirated to 80 µL, and an equal volume of CellTiter-Glo
329 Luminescent Cell Viability Assay reagent (Promega G7571) was added. Luciferase activity was
330 measured using a BioTek Cytation 3 equipped with Gen5 software (v3.08). Each assay was

331 repeated with two technical replicates within two independent biological replicates. Statistical
332 analyses were performed using Prism 10 (GraphPad Software, Inc.). Dose-response inhibition
333 curves for host cell toxicity (CC_{50} values) were generated using the "Log(inhibitor) vs
334 normalized response variable slope" function. The reported values represent averages from three
335 biological replicates.
336 **Ex-vivo Bradyzoite differentiation assay.** CBA/CaJ mice (Strain # 000654) from Jackson
337 Laboratory were housed in an approved facility at Washington University School of Medicine,
338 and all animal studies followed ethical guidelines approved by the Institutional Animal Care and
339 Use Committee. CBA/CaJ mice were infected by oral gavage with 5-10 tissue cysts from the
340 brain homogenate of previously infected mice. The brains of CBA/CaJ mice infected with the
341 TgME49-EW strain [46] were collected at 1-2 mos post-infection, homogenized, and tissue cysts
342 were isolated using Percoll gradients, as described previously [50]. To release the bradyzoites from
343 the tissue cysts, purified tissue cysts were treated with an acid-pepsin solution (170 mM NaCl,
344 60 mM HCl), and a freshly prepared pepsin solution (0.1 mg/mL in 1xPBS) for 10 min at 37 °C.
345 The reaction was stopped by adding a neutralization buffer (94 mM Na_2CO_3). The liberated
346 bradyzoites were then evenly distributed into a duplicate set of 6-well plates (technical
347 replicates), each containing 5 mL of culture media. Each plate included a negative control (media
348 with 0.1% DMSO), the previously characterized PheRS inhibitor BRD7929 (0.5 μM)[33], and
349 pyrimethamine (2.0 μM). Compounds were tested at EC_{90} and $3XEC_{90}$ concentrations based on
350 their corresponding in vitro tachyzoite growth inhibition ($TgEC_{50}$) assays (Table S3). After a 4 hr
351 treatment, the compounds were removed from one set of plates by washing with 3 times in PBS
352 and replacement with compound-free D10 medium. The plates were then incubated at 37ºC, 5%
353 CO_2 undisturbed for 12-14 days to form plaques. Plaque quantification was performed by fixing
354 the plates in 100% ethanol for 5 min at room temperature, followed by staining with a 0.1%
355 crystal violet solution for 10 min. After rinsing with water and air drying, plaque quantification
356 was conducted using a Nikon eclipse ts2 microscope equipped with a 4X objective. The number
357 of plaques from two biological replicates was normalized to DMSO control as a percentage.
358 **Statistical analysis**
359 Statistical comparisons were performed in Prism (GraphPad). Data were first analyzed for
360 normal distribution and according to the outcome, were then non-parametric tests applied.
361 Statistical test and *P* values are given in the figure legends.

Acknowledgments:

We thank Jennifer Barks for HFF cell culture and for providing administrative support for research materials. We acknowledge Maxene Ilagan and Mike Prinsen from Washington University's High Throughput Screening Center for their assistance with assay set-up and data handling. Furthermore, we thank Kaycie Morwood and her team from Calibr – A Division of Scripps Research for their assistance with compound management and plating. The ME49EW was a kindly provided by Michael White, University of South Florida. Partial support provided by an NIH grant (AI143857) and a pilot grant from the Center for Drug Discovery at Washington University (PJ00027513).

Abbreviations used:

DMSO Dimethylsulfoxide

DHFR Dihydrofolate Reductase

EDTA Ethylenediaminetetraacetic acid

HFF Human Foreskin Fibroblasts

HepG2 human hepatocellular carcinoma cell

THP-1 human monocytic tumor cell

HTS High Throughput Screening

nLuc Nano Luciferase

Fluc Firefly Luciferase

PheRS Phenylalanine tRNA synthetase

Supplemental Materials

Table S1 HTS parameters for lines expressing luciferase.

Table S2 HTS parameters for the LOPAC screen.

Table S3 Activity of Primary Hits in growth inhibition assays.

Table S4 Primers used in the study.

Figure S1. Testing of additional TOP HIT compounds for activity against ex vivo bradyzoites.

References

1. Dubey JP. Toxoplasmosis of animals and humans. Boca Raton: CRC Press; 2010. 313 p.
2. Pappas G, Roussos N, Falagas ME. Toxoplasmosis snapshots: global status of *Toxoplasma gondii* seroprevalence and implications for pregnancy and congenital toxoplasmosis. Int J Parasitol. 2009;39(12):1385-94. Epub 2009/05/13. doi: S0020-7519(09)00184-2 [pii] 10.1016/j.ijpara.2009.04.003. PubMed PMID: 19433092.
3. Almeria S, Dubey JP. Foodborne transmission of Toxoplasma gondii infection in the last decade. An overview. Res Vet Sci. 2021;135:371-85. Epub 20201024. doi: 10.1016/j.rvsc.2020.10.019. PubMed PMID: 33148402.
4. Watts E, Zhao Y, Dhara A, Eller B, Patwardhan A, Sinai AP. Novel Approaches Reveal that Toxoplasma gondii Bradyzoites within Tissue Cysts Are Dynamic and Replicating Entities In Vivo. MBio. 2015;6(5):e01155-15. doi: 10.1128/mBio.01155-15. PubMed PMID: 26350965; PMCID: PMC4600105.
5. Elsheikha HM, Marra CM, Zhu XQ. Epidemiology, Pathophysiology, Diagnosis, and Management of Cerebral Toxoplasmosis. Clin Microbiol Rev. 2021;34(1). Epub 20201125. doi: 10.1128/CMR.00115-19. PubMed PMID: 33239310; PMCID: PMC7690944.
6. Torgerson PR, Mastroiacovo P. The global burden of congenital toxoplasmosis: a systematic review. Bull World Health Organ. 2013;91(7):501-8. Epub 2013/07/05. doi: 10.2471/BLT.12.111732 BLT.12.111732 [pii]. PubMed PMID: 23825877; PMCID: 3699792.
7. Jones LA, Alexander J, Roberts CW. Ocular toxoplasmosis: in the storm of the eye. Parasite Immunol. 2006;28:635-42.
8. Glasner PD, Silveira C, Kruszon-Moran D, Martins MC, Burnier M, Silveira S, Camargo ME, Nussenblatt RB, Kaslow RA, Belfort R. An unusually high prevalence of ocular toxoplasmosis in southern Brazil. Am J Opthalmol. 1992;114:136-44.
9. Holland GN. An epidemic of toxoplasmosis: lessons from Coimbatore, India. Arch Ophthalmol. 2010;128(1):126-8. doi: 10.1001/archophthalmol.2008.538. PubMed PMID: 20065229.
10. Palanisamy M, Madhavan B, Balasundaram MB, Andavar R, Venkatapathy N. Outbreak of ocular toxoplasmosis in Coimbatore, India. Indian J Ophthalmol. 2006;54(2):129-31. doi: 10.4103/0301-4738.25839. PubMed PMID: 16770035.
11. Pfaff AW, de-la-Torre A, Rochet E, Brunet J, Sabou M, Sauer A, Bourcier T, Gomez-Marin JE, Candolfi E. New clinical and experimental insights into Old World and neotropical ocular toxoplasmosis. Int J Parasitol. 2013. Epub 2013/11/10. doi: S0020-7519(13)00255-5 [pii] 10.1016/j.ijpara.2013.09.007. PubMed PMID: 24200675.
12. McPhillie M, Zhou Y, El Bissati K, Dubey J, Lorenzi H, Capper M, Lukens AK, Hickman M, Muench S, Verma SK, Weber CR, Wheeler K, Gordon J, Sanders J, Moulton H, Wang K, Kim TK, He Y, Santos T, Woods S, Lee P, Donkin D, Kim E, Fraczek L, Lykins J, Esaa F, Alibana-Clouser F, Dovgin S, Weiss L, Brasseur G, Wirth D, Kent M, Hood L, Meunieur B, Roberts CW, Hasnain SS, Antonyuk SV, Fishwick C, McLeod R. New paradigms for understanding and step changes in treating active and chronic, persistent apicomplexan infections. Sci Rep. 2016;6:29179. Epub 2016/07/15. doi: 10.1038/srep29179. PubMed PMID: 27412848; PMCID: PMC4944145.
13. Xiao J, Savonenko A, Yolken RH. Strain-specific pre-existing immunity: A key to understanding the role of chronic Toxoplasma infection in cognition and Alzheimer's

436 diseases? Neurosci Biobehav Rev. 2022;137:104660. Epub 20220409. doi:
437 10.1016/j.neubiorev.2022.104660. PubMed PMID: 35405182.
438 14. Wei HX, Wei SS, Lindsay DS, Peng HJ. A Systematic Review and Meta-Analysis of the
439 Efficacy of Anti-Toxoplasma gondii Medicines in Humans. PLoS One.
440 2015;10(9):e0138204. Epub 2015/09/24. doi: 10.1371/journal.pone.0138204. PubMed
441 PMID: 26394212; PMCID: PMC4578932.
442 15. McCabe RE. Antitoxoplasma chemotherapy. In: Joynson DHM, Wreghitt TG, editors.
443 Toxoplasmosis: a comprehensive clinical guide. Cambridge: Cambridge Univ. Press; 2001.
444 p. 319-59.
445 16. Ben-Harari RR, Goodwin E, Casoy J. Adverse Event Profile of Pyrimethamine-Based Therapy
446 in Toxoplasmosis: A Systematic Review. Drugs R D. 2017;17(4):523-44. doi:
447 10.1007/s40268-017-0206-8. PubMed PMID: 28879584; PMCID: PMC5694419.
448 17. Alday PH, Doggett JS. Drugs in development for toxoplasmosis: advances, challenges, and
449 current status. Drug Des Devel Ther. 2017;11:273-93. Epub 2017/02/10. doi:
450 10.2147/DDDT.S60973. PubMed PMID: 28182168; PMCID: PMC5279849.
451 18. Kieffer F, Wallon M. Congenital toxoplasmosis. Handb Clin Neurol. 2013;112:1099-101. Epub
452 2013/04/30. doi: 10.1016/B978-0-444-52910-7.00028-3. PubMed PMID: 23622316.
453 19. Berg-Candolfi M, Candolfi E. Depression of the N-demethylation of erythromycin,
454 azithromycin, clarithromycin and clindamycin in murine Toxoplasma infection. Int J
455 Parasitol. 1996;26(11):1321-3. Epub 1996/11/01. PubMed PMID: 9024879.
456 20. Derouin F, Almadany R, Chau F, Rouveix B, Pocidalo JJ. Synergistic activity of azithromycin
457 and pyrimethamine or sulfadiazine in acute experimental toxoplasmosis. Antimicrob
458 Agents Chemother. 1992;36(5):997-1001. Epub 1992/05/01. PubMed PMID: 1324642;
459 PMCID: PMC188824.
460 21. Neville AJ, Zach SJ, Wang X, Larson JJ, Judge AK, Davis LA, Vennerstrom JL, Davis PH.
461 Clinically Available Medicines Demonstrating Anti-Toxoplasma Activity. Antimicrob
462 Agents Chemother. 2015;59(12):7161-9. Epub 2015/09/24. doi: 10.1128/AAC.02009-15.
463 PubMed PMID: 26392504; PMCID: PMC4649158.
464 22. Slimings C, Riley TV. Antibiotics and hospital-acquired Clostridium difficile infection: update
465 of systematic review and meta-analysis. J Antimicrob Chemother. 2014;69(4):881-91.
466 Epub 2013/12/11. doi: 10.1093/jac/dkt477. PubMed PMID: 24324224.
467 23. Benmerzouga I, Checkley LA, Ferdig MT, Arrizabalaga G, Wek RC, Sullivan WJ, Jr.
468 Guanabenz repurposed as an antiparasitic with activity against acute and latent
469 toxoplasmosis. Antimicrob Agents Chemother. 2015;59(11):6939-45. Epub 2015/08/26.
470 doi: 10.1128/AAC.01683-15. PubMed PMID: 26303803; PMCID: PMC4604420.
471 24. Martynowicz J, Doggett JS, Sullivan WJ, Jr. Efficacy of Guanabenz Combination Therapy
472 against Chronic Toxoplasmosis across Multiple Mouse Strains. Antimicrob Agents
473 Chemother. 2020;64(9). Epub 20200820. doi: 10.1128/AAC.00539-20. PubMed PMID:
474 32540979; PMCID: PMC7449173.
475 25. Martynowicz J, Sullivan WJ, Jr. Rebound of cyst number following discontinuation of
476 guanabenz treatment for latent toxoplasmosis. Mol Biochem Parasitol. 2021;245:111411.
477 Epub 20210904. doi: 10.1016/j.molbiopara.2021.111411. PubMed PMID: 34492239;
478 PMCID: PMC8484070.
479 26. Dittmar AJ, Drozda AA, Blader IJ. Drug Repurposing Screening Identifies Novel Compounds
480 That Effectively Inhibit Toxoplasma gondii Growth. mSphere. 2016;1(2). Epub 20160302.
481 doi: 10.1128/mSphere.00042-15. PubMed PMID: 27303726; PMCID: PMC4894684.

27. Soête M, Fortier B, Camus D, Dubremetz JF. *Toxoplasma gondii*: kinetics of bradyzoite-tachyzoite interconversion *in vitro*. Exp Parasitol. 1993;76:259-64.
28. Garfoot AL, Wilson GM, Coon JJ, Knoll LJ. Proteomic and transcriptomic analyses of early and late-chronic Toxoplasma gondii infection shows novel and stage specific transcripts. BMC Genomics. 2019;20(1):859. Epub 2019/11/16. doi: 10.1186/s12864-019-6213-0. PubMed PMID: 31726967; PMCID: PMC6857164.
29. Bohne W, Heeseman J, Gross U. Coexistence of hetergeneous populations of *Toxoplasma gondii* parasites within parasitophorous vacuoles of murine macrophages as revealed by a bradyzoite-specific monoclonal antibody. Parasitol Res. 1993;79:485-7.
30. Smith D, Lunghi M, Olafsson EB, Hatton O, Di Cristina M, Carruthers VB. A High-Throughput Amenable Dual Luciferase System for Measuring Toxoplasma gondii Bradyzoite Viability after Drug Treatment. Anal Chem. 2023;95(2):668-76. Epub 20221222. doi: 10.1021/acs.analchem.2c02174. PubMed PMID: 36548400; PMCID: PMC9850410.
31. Christiansen C, Maus D, Hoppenz E, Murillo-Leon M, Hoffmann T, Scholz J, Melerowicz F, Steinfeldt T, Seeber F, Blume M. In vitro maturation of Toxoplasma gondii bradyzoites in human myotubes and their metabolomic characterization. Nat Commun. 2022;13(1):1168. Epub 20220304. doi: 10.1038/s41467-022-28730-w. PubMed PMID: 35246532; PMCID: PMC8897399.
32. Xia J, Fu Y, Huang W, Sibley LD. Constitutive upregulation of transcription factors underlies permissive bradyzoite differentiation in a natural isolate of Toxoplasma gondii. bioRxiv. 2024. Epub 20240228. doi: 10.1101/2024.02.28.582596. PubMed PMID: 38464000; PMCID: PMC10925318.
33. Radke JB, Melillo B, Mittal P, Sharma M, Sharma A, Fu Y, Uddin T, Gonse A, Comer E, Schreiber SL, Gupta AK, Chatterjee AK, Sibley LD. Bicyclic azetidines target acute and chronic stages of Toxoplasma gondii by inhibiting parasite phenylalanyl t-RNA synthetase. Nat Commun. 2022;13(1):459. Epub 2022/01/26. doi: 10.1038/s41467-022-28108-y. PubMed PMID: 35075105; PMCID: PMC8786932 Washington University have applied for a patent (PCT/US2019/051686 listing J.B.R., E.C., B.M. and L.D.S. as inventors) for the use of bicyclic azetidines for antiparasitic therapies. All other authors declare no competing interests.
34. Bohne W, Gross U, Ferguson DJP, Hessemann J. Cloning and characterization of a bradyzoite-specifically expressed gene (*hsp30/bag1*) of *Toxoplasma gondii*, related to genes encoding small heat-shock proteins of plants. Molecular Microbiology. 1995;16(6):1221-30.
35. Shukla A, Olszewski KL, Llinas M, Rommereim LM, Fox BA, Bzik DJ, Xia D, Wastling J, Beiting D, Roos DS, Shanmugam D. Glycolysis is important for optimal asexual growth and formation of mature tissue cysts by Toxoplasma gondii. Int J Parasitol. 2018;48(12):955-68. Epub 2018/09/04. doi: 10.1016/j.ijpara.2018.05.013. PubMed PMID: 30176233.
36. Blume M, Rodriguez-Contreras D, Landfear S, Fleige T, Soldati-Favre D, Lucius R, Gupta N. Host-derived glucose and its transporter in the obligate intracellular pathogen Toxoplasma gondii are dispensable by glutaminolysis. Proc Natl Acad Sci U S A. 2009;106(31):12998-3003. Epub 2009/07/21. doi: 0903831106 [pii]
10.1073/pnas.0903831106. PubMed PMID: 19617561; PMCID: 2722337.

526 37. McFadden DC, Tomavo S, Berry EA, Boothroyd JC. Characterization of cytochrome b from
527 *Toxoplasma gondii* and Q_o domain mutations as a mechanism of atovaquone-resistance.
528 Mol Biochem Parasitol. 2000;108(1):1-12.
529 38. Yildirim A, Ozbilgin A, Yereli K. Antiprotozoal activity of auranofin on Trypanosoma cruzi,
530 Leishmania tropica and Toxoplasma gondii: in vitro and ex vivo study. Trans R Soc Trop
531 Med Hyg. 2023;117(10):733-40. doi: 10.1093/trstmh/trad040. PubMed PMID: 37377375.
532 39. Andrade RM, Chaparro JD, Capparelli E, Reed SL. Auranofin is highly efficacious against
533 Toxoplasma gondii in vitro and in an in vivo experimental model of acute toxoplasmosis.
534 PLoS Negl Trop Dis. 2014;8(7):e2973. Epub 20140731. doi:
535 10.1371/journal.pntd.0002973. PubMed PMID: 25079790; PMCID: PMC4117455.
536 40. Abou-El-Naga IF, Mogahed N. Repurposing auranofin for treatment of Experimental Cerebral
537 Toxoplasmosis. Acta Parasitol. 2021;66(3):827-36. Epub 20210208. doi: 10.1007/s11686-
538 021-00337-z. PubMed PMID: 33555553.
539 41. Riganti C, Gazzano E, Polimeni M, Costamagna C, Bosia A, Ghigo D. Diphenyleneiodonium
540 inhibits the cell redox metabolism and induces oxidative stress. J Biol Chem.
541 2004;279(46):47726-31. Epub 20040909. doi: 10.1074/jbc.M406314200. PubMed PMID:
542 15358777.
543 42. Sun PR, Gao FF, Choi HG, Zhou W, Yuk JM, Kwon J, Lee YH, Cha GH. Dipenyleneiodonium
544 Induces Growth Inhibition of Toxoplasma gondii through ROS Induction in ARPE-19
545 Cells. Korean J Parasitol. 2019;57(2):83-92. Epub 20190430. doi:
546 10.3347/kjp.2019.57.2.83. PubMed PMID: 31104400; PMCID: PMC6526218.
547 43. Yuan J, Johnson RL, Huang R, Wichterman J, Jiang H, Hayton K, Fidock DA, Wellems TE,
548 Inglese J, Austin CP, Su XZ. Genetic mapping of targets mediating differential chemical
549 phenotypes in Plasmodium falciparum. Nat Chem Biol. 2009;5(10):765-71. Epub
550 20090906. doi: 10.1038/nchembio.215. PubMed PMID: 19734910; PMCID:
551 PMC2784992.
552 44. Pandey M, Singh AK, Thakare R, Talwar S, Karaulia P, Dasgupta A, Chopra S, Pandey AK.
553 Diphenyleneiodonium chloride (DPIC) displays broad-spectrum bactericidal activity. Sci
554 Rep. 2017;7(1):11521. Epub 20170914. doi: 10.1038/s41598-017-11575-5. PubMed
555 PMID: 28912539; PMCID: PMC5599662.
556 45. An Z, Muthusami S, Yu JR, Park WY. T0070907, a PPAR gamma inhibitor, induced G2/M
557 arrest enhances the effect of radiation in human cervical cancer cells through mitotic
558 catastrophe. Reprod Sci. 2014;21(11):1352-61. Epub 20140318. doi:
559 10.1177/1933719114525265. PubMed PMID: 24642720; PMCID: PMC4212328.
560 46. Vizcarra EA, Goerner AL, Ulu A, Hong DD, Bergersen KV, Talavera MA, Le Roch K, Wilson
561 EH, White MW. An ex vivo model of Toxoplasma recrudescence reveals developmental
562 plasticity of the bradyzoite stage. mBio. 2023;14(5):e0183623. Epub 2023/09/07. doi:
563 10.1128/mbio.01836-23. PubMed PMID: 37675999; PMCID: PMC10653814.
564 47. Scholer N, Krause K, Kayser O, Muller RH, Borner K, Hahn H, Liesenfeld O. Atovaquone
565 nanosuspensions show excellent therapeutic effect in a new murine model of reactivated
566 toxoplasmosis. Antimicrob Agents Chemother. 2001;45(6):1771-9. PubMed PMID:
567 11353624.
568 48. Singh N, Sharma B. Toxicological Effects of Berberine and Sanguinarine. Front Mol Biosci.
569 2018;5:21. Epub 20180319. doi: 10.3389/fmolb.2018.00021. PubMed PMID: 29616225;
570 PMCID: PMC5867333.

571 49. Huang LJ, Lan JX, Wang JH, Huang H, Lu K, Zhou ZN, Xin SY, Zhang ZY, Wang JY, Dai P,
572 Chen XM, Hou W. Bioactivity and mechanism of action of sanguinarine and its derivatives
573 in the past 10 years. Biomed Pharmacother. 2024;173:116406. Epub 20240308. doi:
574 10.1016/j.biopha.2024.116406. PubMed PMID: 38460366.
575 50. Wang Q, Sibley LD. Assays for Monitoring Toxoplasma gondii Infectivity in the Laboratory
576 Mouse. Methods Mol Biol. 2020;2071:99-116. Epub 2019/11/24. doi: 10.1007/978-1-
577 4939-9857-9_5. PubMed PMID: 31758448.
578

579

580 **Figure Legends**

581

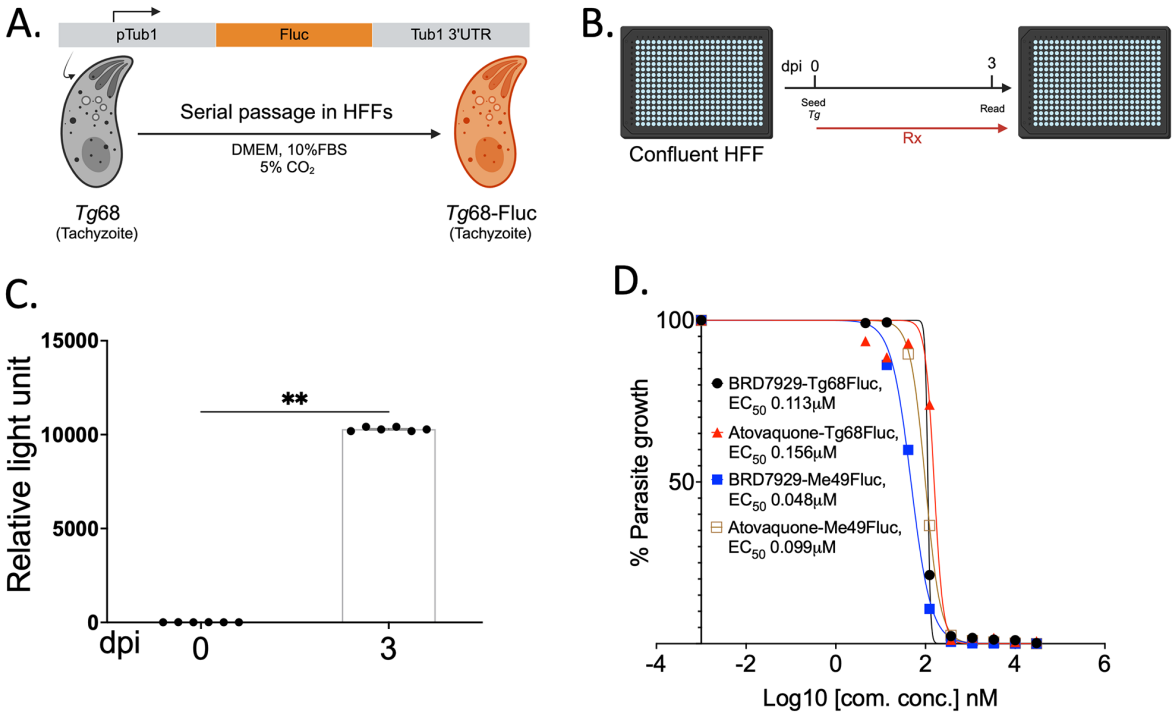

582

583 **Figure 1** Development of a High Throughput Screening assay for growth inhibition of Tg68
584 tachyzoites. (A) A tachyzoite-specific firefly-luciferase (Fluc) reporter strain of Tg68 was
585 generated using the pTUB1 promoter. (B) Confluent HFF cells in 384-well plates were infected
586 with Tg68 tachyzoites and luciferase activity was performed on day 3. (C) Replicate of 12 wells
587 from six independent plates was analyzed for luciferase activity. Fluc expression increased more
588 than 1000 fold and was found significantly higher at day 3 hr (72hr) compared to day 0 (4 hr
589 postinfection). Data accumulated from 12 wells, across 6 plates. Mann-Whitney test, $P < 0.02$.
590 (D) EC_{50} determination for Tg68-pTub1:Fluc and ME49-Fluc treated with serial dilutions of
591 BRD7929 or Atovaquone. All EC_{50} values are presented as the mean of three biological
592 replicates (n = 3)

593

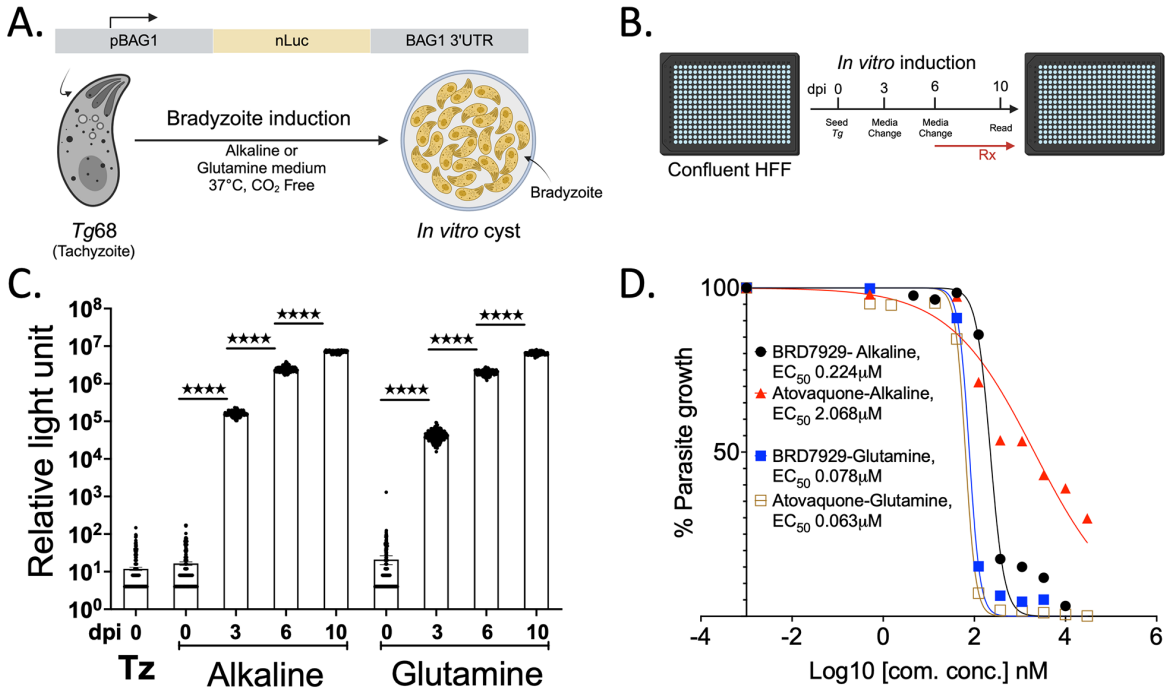

Figure 2 Development of a High Throughput Screening assay for growth inhibition of Tg68 bradyzoites. (A) A bradyzoite-specific Nanoluc luciferase (nLuc) reporter strain of Tg68 was generated using the p*BAG1* promoter. Parasites were grown in alkaline medium (pH 8.2), CO_2 free or in the absence of glucose supplemented with glutamine, which stimulates in vitro development of bradyzoites. (B) Confluent HFFs in 384-well plates were infected with Tg68 tachyzoites for two hr, washed and then cultured either in D10 under normal conditions (Tz) or switch to alkaline or glutamine conditions to induce bradyzoites. The cultures were then maintained under CO_2-free conditions for 10 days with media changes on day 3 and 6, with a compound treatment at day 6 and readout at day 10. (C) Luciferase signals from tachyzoites (Tz) harvested at day 0 (4 hrs postinfection) postinfection or bradyzoites induced for different times (day 0 (4 hr) to day 10) by culture in alkaline or glutamine media. Comparisons between sequential time points using Mann Whitney test, **** $P < 0.0001$(D) Determination of EC_{50} values for BRD7929 and atovaquone treatment of in vitro induced bradyzoites culture in alkaline or glutamine media. All EC_{50} values are presented as the mean of four biological replicates (n = 4).

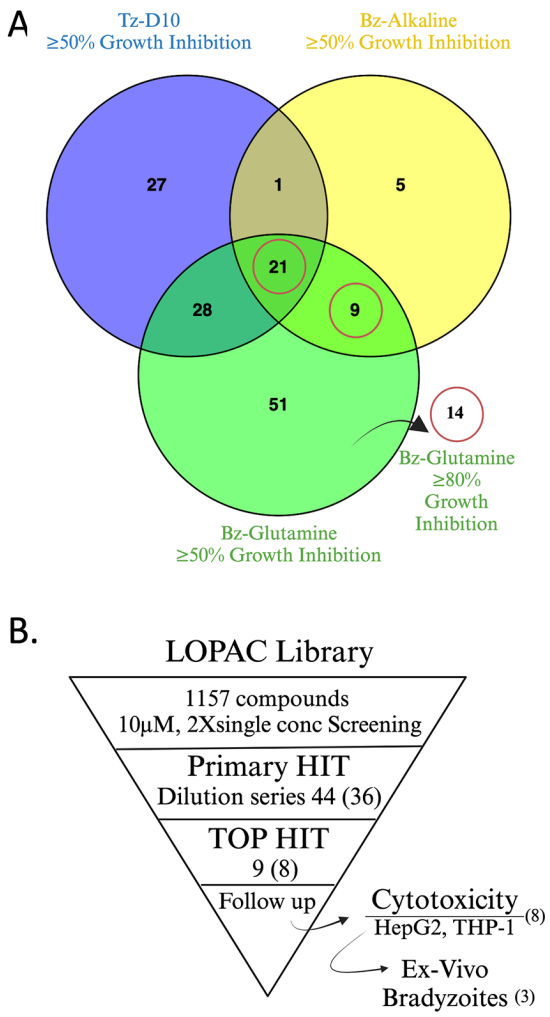

Figure 3 Summary of LOPAC screening for growth inhibition of *T. gondii*. (A) Venn diagram showing the number of compounds with ≥ 50% of growth inhibition at 10 µM in each of three growth assays. Tz = tachyzoite growth assay, Alk = alkaline induced bradyzoite growth assay, Gln = glutamine induced bradyzoite growth assay. Red circled numbers indicate the selection criteria for Primary Hits. (B). Summary of LOPAC screen and prioritization of Hits for follow up. Of 44 Primary Hits, 36 were available for dilution series to determine EC_{50} values. Of 9 Top Hits, 8 were available for further biological testing.

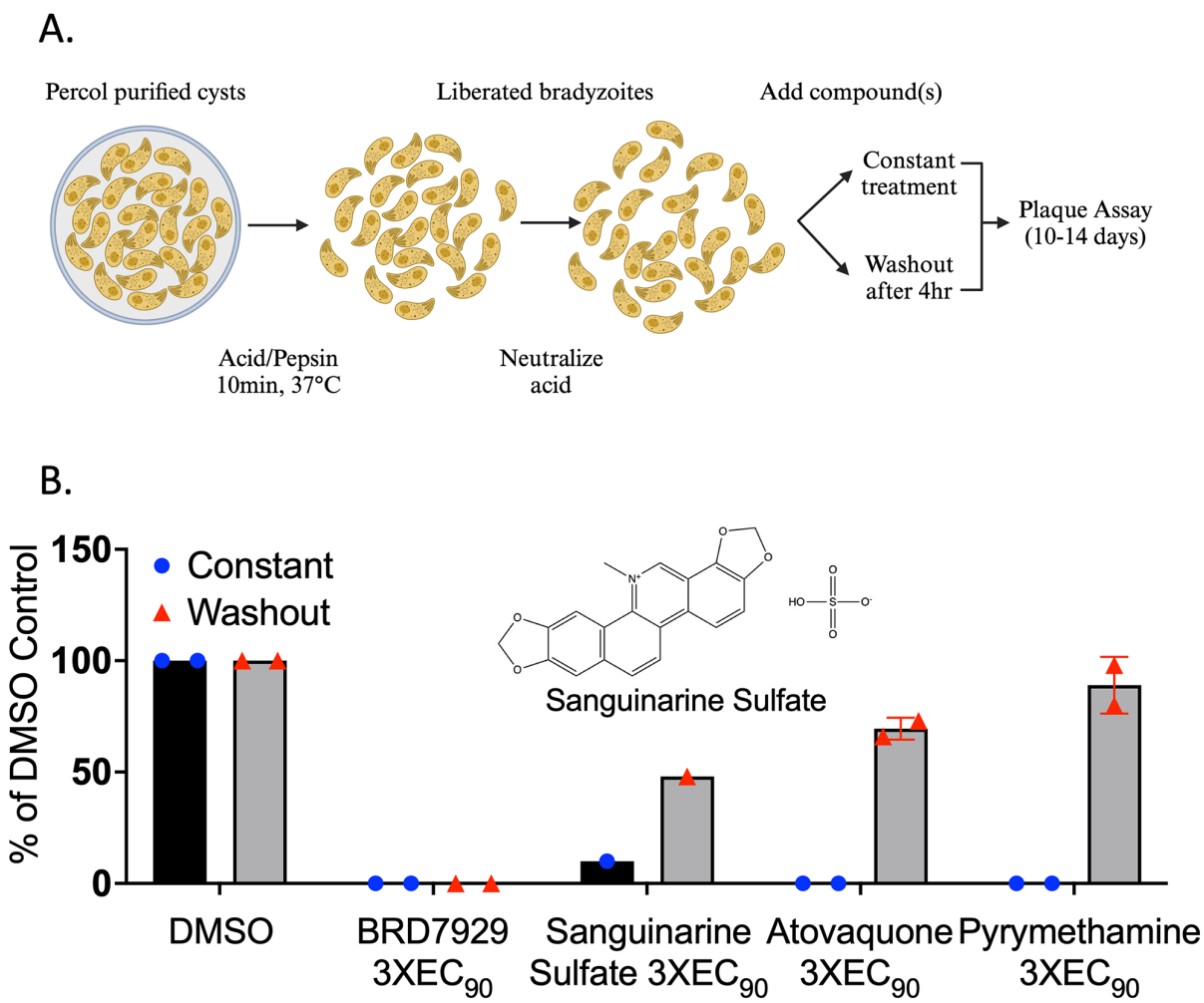

Figure 4. Testing of compounds for activity against ex vivo bradyzoites. (A) Schematic for isolation of bradyzoites from chronically infect mice and testing in vitro during continuous treatment or after 4 hr treatment and washout. (B) Testing of the Top Hit Sanguinarine and reference compounds in continuous treatment vs. 4 hr treatment and washout. Values are determined from plaque counts after 10-14 days of outgrowth and are normalized to the DMSO control for each condition. Compounds were used at $3XEC_{90}$ based on sensitivity of Tg68Fluc tachyzoites (**Table S3)**. Data from 2 biological replicates, bar graph represent the average of percentage of number of plaques in the treatment group normalized to DMSO control.

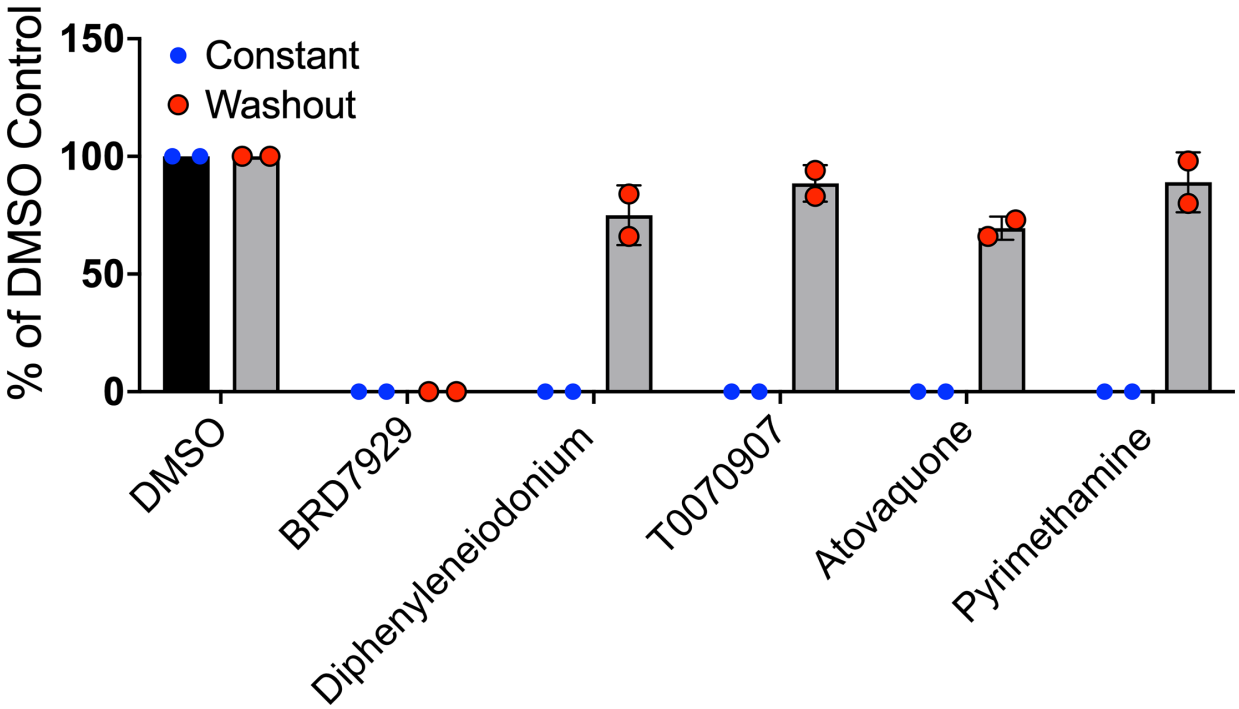

Figure S1. Testing of additional TOP HIT compounds for activity against ex vivo bradyzoites. Plaque number from 2 biological replicates for Diphenyleneiodonium, T0070907 and reference compounds in continuous treatment vs. 4 hr treatment and washout presented in average percentage with standard deviation bar.